Research Article

Zhenjie Ge, Lihua Bai*, Xu Su, and Keying Liu

Nonsequential double ionization channels control of CO_2 molecules with counter-rotating two-color circularly polarized laser field by laser wavelength

https://doi.org/10.1515/phys-2023-0114
received July 16, 2023; accepted September 04, 2023

Abstract: Using the classical ensemble model, we investigate the effect of laser wavelength on the electron dynamics process of nonsequential double ionization (NSDI) for linear triatomic molecules driven by a counter-rotating two-color circularly polarized laser field. Based on the delay time between recollision and final double ionization, two particular ionization channels are separated: recollision-impact ionization (RII) and recollision-induced excitation with subsequent ionization (RESI). Numerical results show that with the increase of the laser wavelength, the triangle structure of the ion momentum distribution becomes more obvious, which indicates that the electron–electron correlation of NSDI is enhanced. In addition, we find that the ratio of the RESI channel gradually decreases with the increase of the laser wavelength, while the ratio of the RII channel is opposite. However, the dominant channel is still RESI. It means that the two ionization channels can be controlled effectively by changing the laser wavelength.

Keywords: linear triatomic molecules, two-color laser fields, nonsequential double ionization, recollision-impact ionization, recollision-induced excitation with subsequent ionization

1 Introduction

With the development of laser technology, the interaction of atoms, molecules, and strong laser fields has generated many interesting nonlinear phenomena, such as above-threshold ionization [1–3], nonsequential double ionization (NSDI) [4–6], and high-order harmonic generation [7]. Theoretical and experimental work has been devoted to observing these physical phenomena. Among them, NSDI in strong field physics has attracted much attention [4,8]. Because the electron–electron correlation plays a significant role in the NSDI process, a large number of studies about NSDI are related to the electron–electron correlation [9], such as angular correlation [10–12] and recollision [13–15].

The NSDI process can be explained by a three-step model [16,17]. First, when an atom or a molecule is exposed to a strong laser field, an electron can be freed by tunneling ionization [18]. Then, the released electron is accelerated by the intense laser field, and it can be driven back to the parent ion when the laser field is reversed [18]. Therefore, the returning electron recollides with the parent ion inelastically, resulting in NSDI [5,6,19]. Due to the recollision of the two electrons during the NSDI process, the two electrons are highly correlated. A large number of theoretical and experimental studies have been performed to explore the correlated dynamics of the two electrons in NSDI. Two recollision mechanisms, recollision-impact ionization (RII) [20,21] and recollision-induced excitation with subsequent ionization (RESI) [22], in the NSDI process have been found. These two recollision mechanisms can be distinguished by the delay time. When the energy of the returning electron is greater than the ionization potential energy of the bound electron, the bound electron will be ionized directly [23,24]. The process for the shorter delay time is defined as RII [18,25]. The bound electron cannot be ionized directly if the energy of the returning electron is less than the ionization potential energy of the bound electron [26,27] and the process for the longer delay time is defined as RESI [18,25].

The development of laser technology has also enabled people to achieve a lot of different laser pulses, such as elliptically polarized (EP) laser pulses, circularly polarized

* **Corresponding author: Lihua Bai**, Department of Physics, College of Sciences, Shanghai University, Shanghai 200444, China, e-mail: lhbai@163.com
Zhenjie Ge, **Xu Su**, **Keying Liu:** Department of Physics, College of Sciences, Shanghai University, Shanghai 200444, China

(CP) laser pulses, and two-color circularly polarized (TCCP) laser pulses [28]. Recently, it has been reported experimentally that the NSDI is studied in counter-rotating two-color circularly polarized (CRTC) laser fields [29–32]. The CRTC laser field is widely used in the research of NSDI due to its special electric field structure. In recent years, Zhang *et al.* have found that the CRTC laser field is beneficial in increasing the double ionization (DI) probability for O_2 molecules [33]. Few-cycle laser pulses can simplify the NSDI process by achieving a single recollision event [21]. It has been found that the relative phase and the polarization of the TCCP laser field can affect the DI probability and the correlation effect [18,34,35]. Currently, we have found that NSDI in the CRTC laser fields for different laser wavelengths has not received much attention.

In this article, we investigate the effect of the laser wavelength of NSDI for CO_2 molecules in the CRTC laser field with a classical ensemble method [36,37]. It is shown that the laser wavelength influences not only the yield of DI but also two particular channels (RII and RESI) in NSDI. In addition, we study the electron–electron correlation in NSDI at different laser wavelengths. Control between the two channels can be achieved by varying the laser wavelength.

2 Theoretical model

In this work, we apply the two-dimensional (2D) classical ensemble model to investigate the effect of the laser wavelength in NSDI by the CRTC laser field. The classical ensemble model has been widely used in strong laser field electron dynamics. The underlying recollision processes and mechanisms in NSDI can be presented intuitively by tracing the classical trajectories [38,39].

In our calculation, the CO_2 molecule is arranged on the x-axis. The two oxygen atoms are placed at coordinates $(-R,0)$ and $(R,0)$. The Hamiltonian of the CO_2 molecules without an electric field can be written as follows (in atomic units):

$$H_e = T(\boldsymbol{p}_i) + V(\boldsymbol{r}_i), \tag{1}$$

where the kinetic energy T and potential energy V of the CO_2 molecules can be represented as follows:

$$T(\boldsymbol{p}_i) = \sum_{i=1,2} \frac{\boldsymbol{p}_i^2}{2}, \tag{2}$$

$$\begin{aligned} V(\boldsymbol{r}_i) = &- \sum_{i=1,2} \frac{2/3}{\sqrt{x_i^2 + y_i^2 + a_c^2}} \\ &- \sum_{i=1,2} \frac{2/3}{\sqrt{(x_i - R)^2 + y_i^2 + a_o^2}} \\ &- \sum_{i=1,2} \frac{2/3}{\sqrt{(x_i + R)^2 + y_i^2 + a_o^2}} \\ &+ \frac{1}{\sqrt{(x_1 - x_2)^2 + (y_1 - y_2)^2 + b^2}}, \end{aligned} \tag{3}$$

the Hamiltonian of the CO_2 molecules is the total energy without an external electric field (the sum of the first ionization potential energy and the second ionization potential energy). Here, $\boldsymbol{p}_i$ and $\boldsymbol{r}_i$ represent the momentum and the position of the two electrons [34]. The internuclear $R = 2.19$ a.u.. In this article, $a_c = 1$, $a_o = 0.8$, and $b = 0.05$ (a_c and a_o are the softcore coefficients used to adjust the bond potential of the atom, shielding the attraction of the atomic nucleus to electrons, and b is the softcore coefficient used to adjust the Coulomb potential between electrons, that is, the Coulomb repulsion of electrons to electrons). Then, we switch on the external laser field. The Hamiltonian of the two electrons in the laser field is expressed as follows:

$$H = H_e + (\boldsymbol{r}_1 + \boldsymbol{r}_2)\cdot \boldsymbol{E}(t), \tag{4}$$

where $\boldsymbol{E}(t) = \boldsymbol{E}_r(t) + \boldsymbol{E}_b(t)$ is the CRTC laser field, where $\boldsymbol{E}_r(t)$ is the fundamental (red) laser pulse, and $\boldsymbol{E}_b(t)$ is the second harmonic (blue) laser pulse [28]. It is expressed as follows:

$$\boldsymbol{E}_r(t) = \frac{E_0}{1 + \gamma_E} f(t)[\cos(\omega_r t)\boldsymbol{x} + \sin(\omega_r t)\boldsymbol{y}], \tag{5}$$

$$\boldsymbol{E}_b(t) = \frac{\gamma_E E_0}{1 + \gamma_E} f(t)[\cos(\omega_b t)\boldsymbol{x} - \sin(\omega_b t)\boldsymbol{y}]. \tag{6}$$

With the maximum combined electric field amplitude E_0, γ_E is equal to 1, which means that the laser intensities of two CP laser fields are the same. ω_r is the fundamental frequency (corresponding to the laser wavelength of the fundamental laser field), and ω_b is the second harmonic frequency (corresponding to the laser wavelength of the second harmonic laser field). $f(t) = \sin^2(\pi t/NT)$ is the pulse envelope function. T is an optical cycle (o.c.), and the number of optical cycles is four optical cycles ($N = 4$). The motion of two electrons in the laser field needs to solve Hamilton's equations, which is written as follows:

$$\frac{\mathrm{d}\boldsymbol{r}_i}{\mathrm{d}t} = \frac{\partial H}{\partial p_i}, \frac{\mathrm{d}\,\boldsymbol{p}_i}{\mathrm{d}\,t} = -\frac{\partial H}{\partial r_i}. \tag{7}$$

The aforementioned equations can be solved by the standard fourth to fifth Runge–Kutta algorithm. In order to ensure that the total energy is positive, the initial positions and momentum distributions of the two electrons satisfy the Gaussian distribution. Then, let the electrons evolve freely for a long enough time (100 a.u.) to obtain the initial ensemble when the electron position and momentum distribution are stable after getting a stable initial ensemble through screening. Then, the laser field is added, and all electrons begin to evolve under the action of the Coulomb potential and electric field until the pulse finishes. If the total energy of the two electrons is greater than zero at the end of the pulse, a DI event is recorded [29].

3 Results and discussion

In order to obtain the maximum recollision, we investigate the DI probability of CO_2 molecules as a function of the laser intensity in the CRTC laser field with different laser wavelengths, as shown in Figure 1. We can find the "knee" structure, which means a significant electron–electron correlation effect in NSDI. The DI probability is changed with different laser wavelengths under a certain laser intensity,

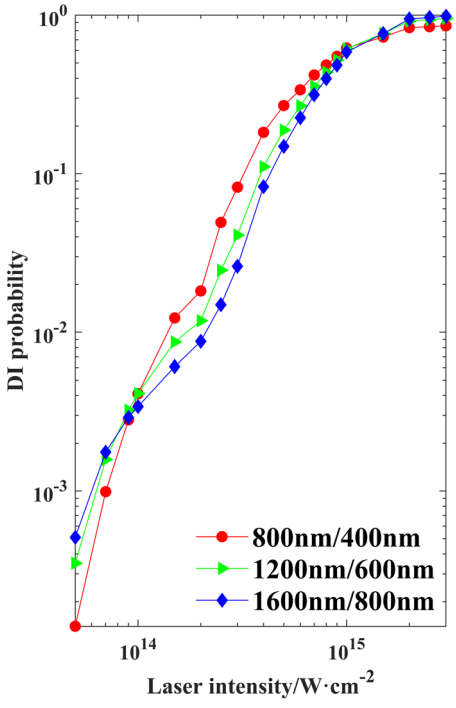

Figure 1: The DI probability of CO_2 molecules as a function of the laser intensity in the CRTC laser field. The curves of red circle, green triangle, and blue square represent laser fields at laser wavelengths of 800 nm/400 nm, 1,200 nm/600 nm, and 1,600 nm/800 nm, respectively.

which indicates that the laser wavelength can affect the DI probability of CO_2 molecules in the few-cycle CRTC laser field. However, it is a little bit different for linearly polarized and EP laser fields [21,40] because their curves of DI probability *versus* laser intensity twist together. Meanwhile, we choose the laser field intensity of $I_0 = 2 \times 10^{14}$ W/cm^2.

One of the important significances of NSDI is to explore the electron–electron correlation. Since there is no simple and clear polarized direction for the CRTC laser field, we explore the correlation between two electrons through recoil momentum distributions of the ion [18]. Because the net momentum of the electroneutral ion-electron system is zero, the relationship $\boldsymbol{P}_{CO_2^{2+}} = -(\boldsymbol{P}_{e1} + \boldsymbol{P}_{e2})$ can be obtained [29]. Therefore, Figure 2 shows the ion momentum distribution of CO_2 molecules under different laser wavelengths in CRTC laser fields at the laser intensity 2×10^{14} W/cm^2. We can find that the shape of the negative vector potential of the electric field is a triangle structure. The shape of the ion momentum distribution is consistent with the shape of the negative vector potential of the electric field. Similar structures have been extensively studied both experimentally and theoretically [19,22]. In these studies, the results and analysis show that the RII is an important reason for the structure. Therefore, the RII forms ion momentum distributions far from the origin due to the short delay time and strong electron–electron correlation. The RESI forms ion momentum distributions near the origin due to the long delay time and weak electron–electron correlation. Figure 2 also shows that the ion momentum distribution gradually spreads out from the origin as the laser wavelength increases, which allows us to infer that the ionization channel has been changed. We will continue to analyze the details and separate the ionization channels by the delay time.

We investigate the DI time (t_{DI}) and the recollision time (t_{RC}) in the CRTC laser field with different laser wavelengths. When the recollision of the two electrons occurs, the Coulomb repulsion energy increases instantaneously [21]. We define t_{RC} as the moment when the Coulomb potential energy between two electrons reaches its maximum [18]. Since the two electrons are indistinguishable, we define the final ionized electron as the second ionized electron after the recollision. Therefore, the corresponding t_{DI} is defined as the second ionization moment after the recollision. The delay time (t_{DI}–t_{RC}) is defined as the time interval between the recollision and the final DI [21,40].

Figure 3 shows that t_{DI} *versus* t_{RC} for different laser wavelengths in CRTC laser fields. The white diagonals of the pictures represent the moments when t_{DI} and t_{RC} are equal, and regions close to the white diagonal are marked by red dashed boxes. Therefore, the part far from the white diagonal means that the delay time is longer, corresponding

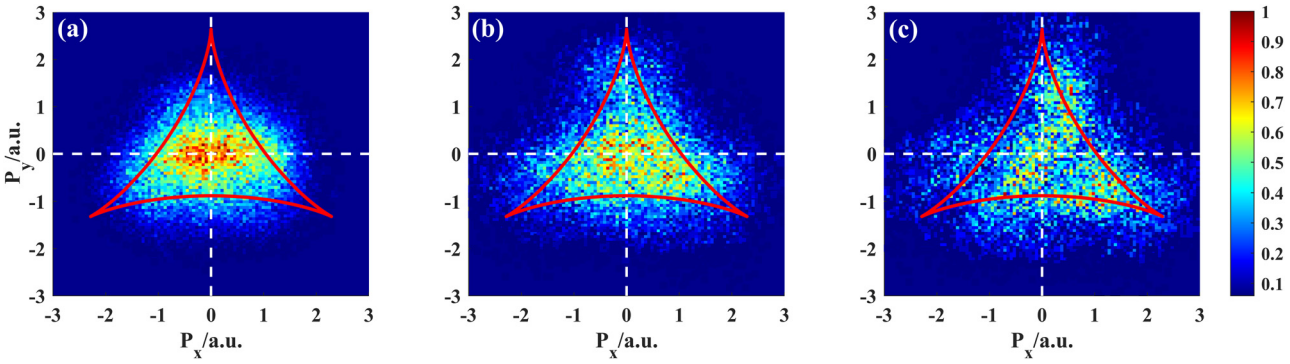

Figure 2: Ion momentum distributions in the CRTC laser field. The laser intensity is 2×10^{14} W/cm^2, and the laser wavelengths are chosen as (a) 800 nm/400 nm, (b) 1,200 nm/600 nm, and (c) 1,600 nm/800 nm, respectively. The solid red line represents the negative vector potential $-\boldsymbol{A}(t)$ of the CRTC laser field.

to the RESI channel, whereas the part near the white diagonal means that the delay time is shorter, corresponding to the RII channel. As shown in Figure 3(a), when the laser wavelength of the combined laser field is 800 and 400 nm, the whole cluster is far away from the diagonal, and the proportion of the time distribution in the red dashed box is about 17.15%. As shown in Figure 3(b), when the laser wavelength of the combined laser field is 1,200 and 600 nm, the whole cluster is close to the diagonal, and the proportion of the time distribution in the red dashed box rises to 24.22%, which means that the delay time and the ionization channel have been changed. In Figure 3(c), we can also see that more of the whole cluster is close to the diagonal when the laser wavelength of the combined laser field is 1,600 and 800 nm, and the proportion of the time distribution in the red dashed box rises to 33.46%. From Figure 3, we can conclude that the laser wavelength will affect t_{DI} and t_{RC}. The underlying mechanism of t_{DI} versus t_{RC} means more RII channels and fewer RESI channels.

Figure 4 shows the counts of the delay-time distribution with different laser wavelengths in CRTC laser fields. We can find that the counts of delay time reach their first minimum around 0.12o.c–0.2o.c. with the increase of the laser wavelength, which clearly separates shorter and longer delay time [21,40]. Therefore, we define the RESI channel with a delay time between recollision and final DI longer than 0.16o.c. The others with a shorter delay time are classified as the RII channel.

The ion momentum distributions shown in Figure 2 can be separated into two ion momentum distributions (RESI and RII). Figure 5 shows the ion momentum distribution of RESI (RII) with the increase of the laser wavelength in the CRTC laser field at the laser intensity of 2×10^{14} W/cm^2. In Figure 2, the ion momentum distributions consist of two parts: the ion momentum distributions of the RESI channel and the ion momentum distributions of the RII channel. We simulate the above two parts separately and then obtain the ion momentum distributions ionized by the RESI channel, as shown in Figure 5(a)–(c), and the ion momentum distributions ionized by the RII channel, as shown in Figure 5(d)–(f). As shown in Figure 5(a)–(c), although the ion momentum distributions of RESI gradually diffuse to the surroundings

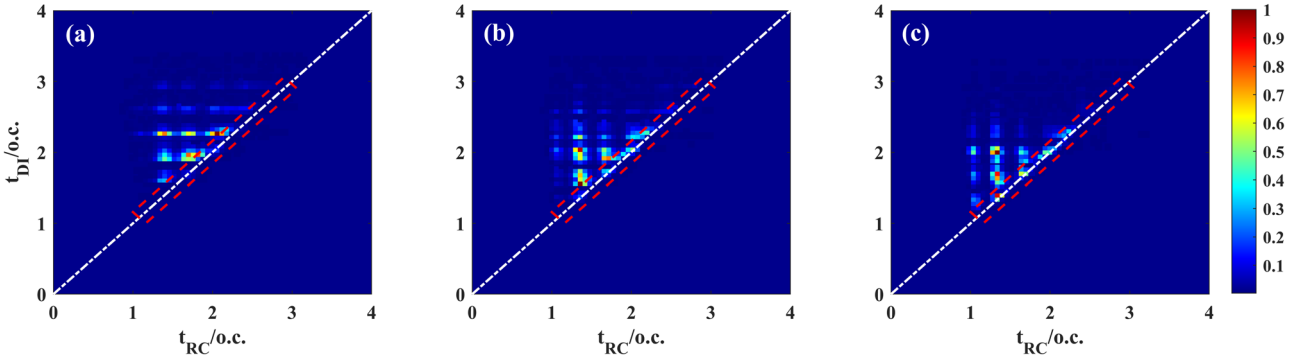

Figure 3: The DI time (t_{DI}) *versus* the recollision time (t_{RC}) for different laser wavelengths in the CRTC laser field. The laser intensity is 2×10^{14} W/cm^2, and the laser wavelengths are chosen as (a) 800 nm/400 nm, (b) 1,200 nm/600 nm, and (c) 1,600 nm/800 nm, respectively.

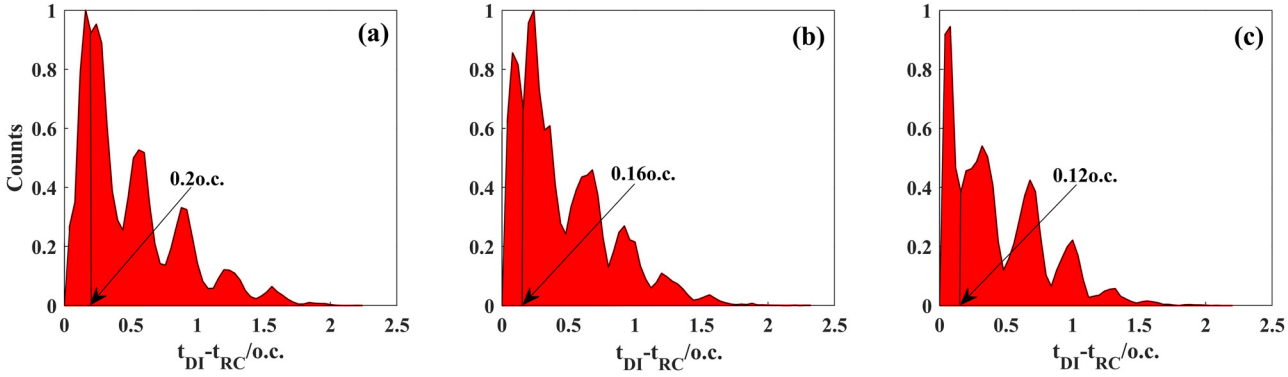

Figure 4: Counts of the delay time for different laser wavelengths in the CRTC laser field. The laser intensity is 2×10^{14} W/cm^2, and the laser wavelengths are chosen as (a) 800 nm/400 nm, (b) 1,200 nm/600 nm, and (c) 1,600 nm/800 nm, respectively. The RII and RESI channels can be distinguished by the first minimum of the statistic results.

with the increase of the laser wavelength, they are still mainly distributed in the central area of the triangular structure. This is because when the first electron is ionized, the second electron is not ionized immediately. Therefore, it means a weak electron–electron correlation in NSDI. In Figure 5(d)–(f), we can see that the ion momentum distributions of RII are mainly distributed in the edge region of the triangular structure with the increase of the laser wavelength. In this case, two electrons are ionized from the core at almost the same time. And it means a strong electron–electron correlation in NSDI.

To distinguish the RESI channel and RII channel clearly, Figure 6 shows the typical energy trajectories in the combined laser field of 800 and 400 nm. Among them, the black solid line is the repulsion energy of two electrons, and the red dashed line and the blue dotted line are the energies of the two electrons, respectively. In Figure 6, the recollision occurs when the repulsion energy is maximum. From Figure 6(a),

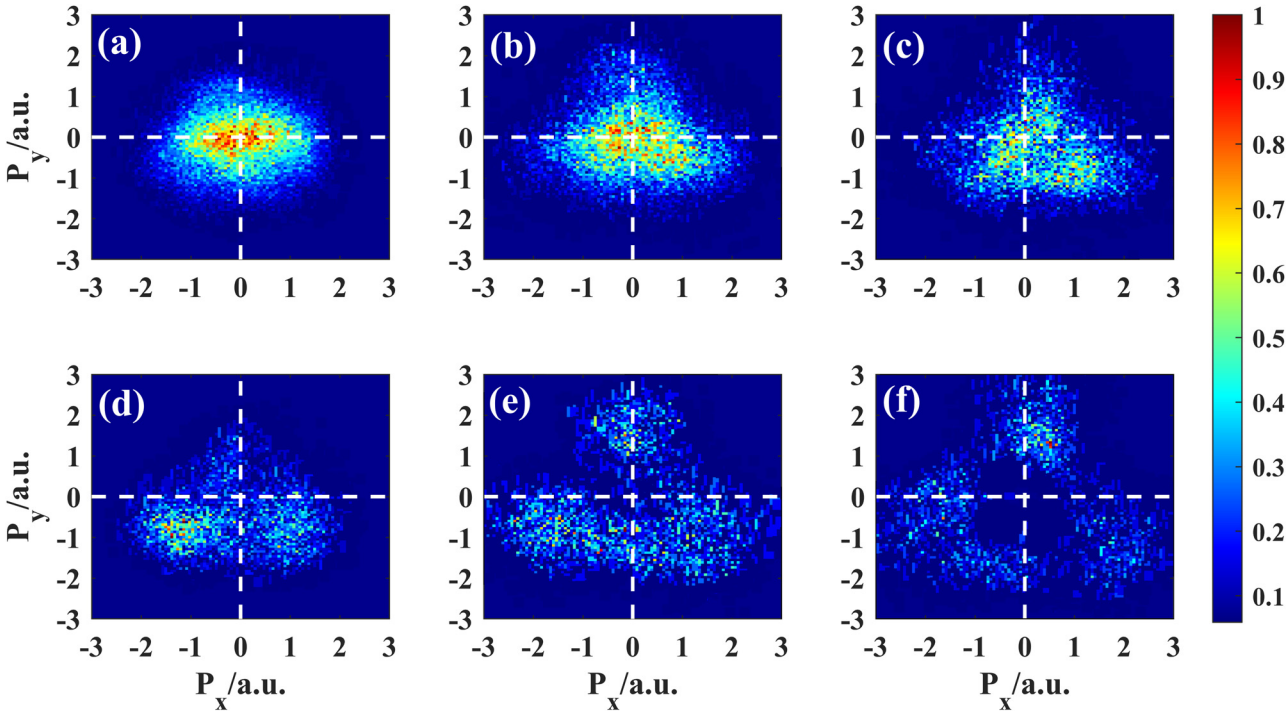

Figure 5: Ion momentum distributions for different laser wavelengths in the CRTC laser field. The laser intensity is 2×10^{14} W/cm^2, and the laser wavelengths are chosen as (a) and (d) 800 nm/400 nm, (b) and (e) 1,200 nm/600 nm, and (c) and (f) 1,600 nm/800 nm, respectively. The upper row shows the RESI channel, and the lower row shows the RII channel.

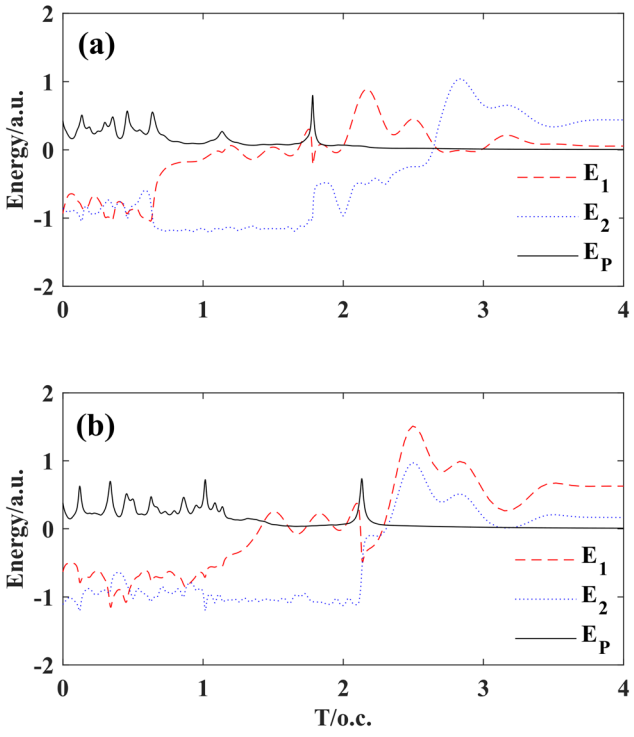

Figure 6: Two typical energy trajectories of (a) RESI channel and (b) RII channel. The laser wavelength is 800 nm/400 nm, and the laser intensity is 2×10^{14} W/cm^2. The black solid line marks the repulsion energy between the two electrons. The red dashed line and blue dotted line mark the energies of the two electrons, respectively.

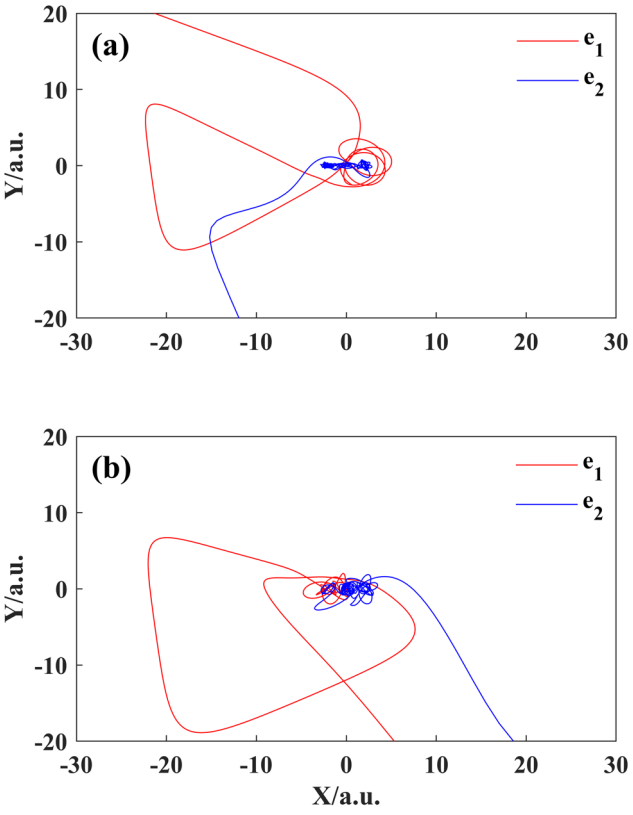

Figure 7: The trajectory of the two electrons in the 2D plane for (a) the RESI channel and (b) the RII channel. The laser wavelength is 800 nm/400 nm, and the laser intensity is 2×10^{14} W/cm^2. The red curve represents the trajectory of the returning electron, and the blue curve represents the trajectory of the bound electron.

we can find that the energy of the returning electron is greater than zero, and the bound electron oscillates at the excited bound state after recollision. Then, the DI occurs at the maximum of the field (the energy of both electrons is greater than zero). There is a longer delay time in this process, corresponding to the RESI. From Figure 6(b), we can find that two electrons are ionized directly after recollision (the energy of both electrons is greater than zero), which means that the returning electron collides strongly with the bound electron and transfers enough energy to make the bound electron ionized. The delay time is shorter in this process, corresponding to the RII.

In addition, the delay time is different in the two ionization channels, so there must be different trajectories. Figure 7 shows two typical classical trajectories in the combined laser field of 800 and 400 nm. Among them, the red solid line represents the trajectory of the returning electron, and the blue solid line represents the trajectory of the bound electron. In Figure 7(a), we can see that the returning electron has a shorter trajectory in the CRTC laser field, and then it collides with the bound electron. At this time, the bound electron oscillates at the excited bound state. The bound electrons ionize in the opposite direction to that of the returning electrons after a period of time. It corresponds to the RESI in Figure 6(a). However, in Figure 7(b), we can see that the returning electron has a longer trajectory in the CRTC laser field, then the returning electron collides with the bound electron. Due to the shorter delay time, both electrons are ionized in the same direction. It corresponds to the RII in Figure 6(b).

Finally, we discuss the ratio of the two ionization channels in the total ionization channels as the laser wavelength increases. We define the ratio of the RESI as $N_{\mathrm{RESI}}/(N_{\mathrm{RESI}} + N_{\mathrm{RII}})$ and the ratio of the RII as $N_{\mathrm{RII}}/(N_{\mathrm{RESI}} + N_{\mathrm{RII}})$. N_{RESI} and N_{RII} are the counts of RESI and RII. In Figure 8, we can see that when the laser wavelength of the combined laser field is 400 and 200 nm, the ratio of the RESI channel is much higher than the ratio of the RII channel. We can also see that the two ionization channels show different trends with the change in the laser wavelength. As the laser wavelength increases, the ratio of the RESI channel decreases gradually while the ratio of the RII channel increases gradually. It means that the two channels can be controlled effectively by changing the laser wavelength. In addition, we find that although the

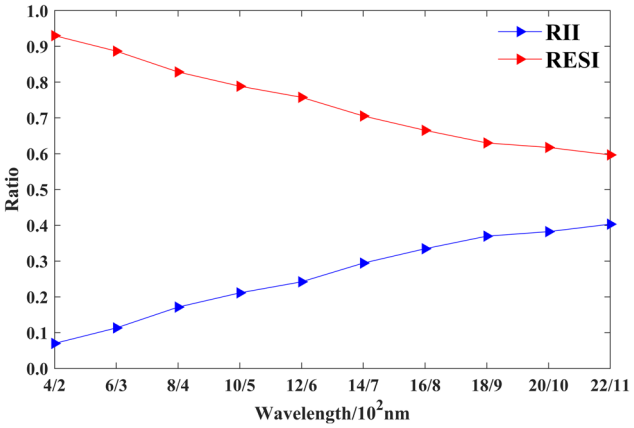

Figure 8: Ratio between different ionization channels and total ionization *versus* laser wavelengths. The laser intensity is 2×10^{14} W/cm^2, and the dominance of the RESI is obvious.

RII channel increases with the increase of the laser wavelength, the dominant channel is still RESI.

4 Conclusions

In conclusion, the two ionization channels in NSDI of CO_2 molecules in the few-cycle CRTC laser field are investigated with the 2D classical ensemble model. The numerical results show that the shape of the ion momentum distribution is consistent with the shape of the negative vector potential of the CRTC laser field, and the ion momentum distribution gradually spreads out from the origin as the laser wavelength increases. In addition, the delay time decreases gradually with the increase of the laser wavelength, but the electron–electron correlation is stronger. To further investigate the effect of the laser wavelength, we separate the ion momentum distribution of the RII channel and the RESI channel by the delay time. Finally, the ratio of the two ionization channels can be influenced by the laser wavelength, while the dominance of the RESI channel is obvious. This article further complemented the research of the NSDI electron dynamics process of linear triatomic molecules in CRTC laser fields, and the results also provide references to explore the electron–electron correlation in experiments.

Funding information: The authors state no funding involved.

Author contributions: All authors have accepted responsibility for the entire content of this manuscript and approved its submission.

Conflict of interest: The authors state no conflict of interest.

References

[1] Paulus GG, Nicklich W, Xu H, Lambropoulos P, Walther H. Plateau in above threshold ionization spectra. Phys Rev Lett. 1994;72(18):2851–4.
[2] Agostini P, Fabre F, Mainfray G, Petite G, Rahman NK. Free-free transitions following six-photon ionization of xenon atoms. Phys Rev Lett. 1979;42(17):1127–30.
[3] Kruit P, Kimman J, Muller HG, van der Wiel MJ. Electron spectra from multiphoton ionization of xenon at 1064, 532, and 355 nm. Phys Rev A. 1983;28(1):248–55.
[4] Song KL, Yu WW, Ben S, Xu TT, Zhang HD, Guo PY, et al. Theoretical study on non-sequential double ionization of carbon disulfide with different bond lengths in linearly polarized laser fields. Chin Phys B. 2017;26(2):023204.
[5] Walker B, Sheehy B, DiMauro LF, Agostini P, Schafer KJ, Klander KC. Precision measurement of strong field double ionization of helium. Phys Rev Lett. 1994;73(9):1227–30.
[6] Fittinghoff DN, Bolton PR, Chang B, Kulander KC. Observation of nonsequential double ionization of helium with optical tunneling. Phys Rev Lett. 1992;69(18):2642–5.
[7] Krausz F, Ivanov M. Attosecond physics. Rev Mod Phys. 2009;81(1):163–234.
[8] Li HY, Wang B, Chen J, Jiang HB, Li XF, Liu J, et al. Effects of a static electric field on nonsequential double ionization. Phys Rev A. 2007;76(3):033405.
[9] Becker W, Liu X, Ho PJ, Eberly JH. Theories of photoelectron correlation in laser-driven multiple atomic ionization. Rev Mod Phys. 2012;84(3):1011–43.
[10] Fleischer A, Wörner HJ, Arissian L, Liu LR, Meckel M, Pippert A, et al. Probing angular correlations in sequential double ionization. Phys Rev Lett. 2011;107(11):113003.
[11] Wang X, Tian J, Eberly JH. Angular correlation in strong-field double ionization under circular polarization. Phys Rev Lett. 2013;110(7):073001.
[12] Guo J, Wang T, Liu XS, Sun JZ. Non-sequential double ionization of Mg atoms in elliptically polarized laser fields. Laser Physics. 2013;23(5):055303.
[13] Mauger F, Chandre C, Uzer T. Recollisions and correlated double ionization with circularly polarized light. Phys Rev Lett. 2010;105(8):083002.
[14] Fu LB, Xin GG, Ye DF, Liu J. Recollision dynamics and phase diagram for nonsequential double ionization with circularly polarized laser fields. Phys Rev Lett. 2012;108(10):103601.
[15] Hao XL, Wang GQ, Jia XY, Li WD. Nonsequential double ionization of Ne in an elliptically polarized intense laser field. Phys Rev A. 2009;80(2):023408.
[16] Corkum PB. Plasma perspective on strong field multiphoton ionization. Phys Rev Lett. 1993;71(13):1994–7.
[17] Kulander KC, Cooper J, Schafer KJ. Laser-assisted inelastic rescattering during above-threshold ionization. Phys Rev A. 1995;51(1):561–8.
[18] Chen JH, Xu TT, Han T, Sun Y, Xu QY, Liu XS. Relative phase effect of nonsequential double ionization in Ar by two-color elliptically polarized laser field. Chin Phys B. 2020;29(1):013203.
[19] Huang C, Zhou Y, Zhang Q, Lu P. Contribution of recollision ionization to the cross-shaped structure in nonsequential double ionization. Opt Express. 2013;21(9):11382.

[20] Ye DF, Liu J. Strong-field double ionization at the transition to below the recollision threshold. Phys Rev A. 2010;81(4):043402.
[21] Ben S, Wang T, Xu TT, Guo J, Liu XS. Nonsequential double ionization channels control of Ar with few-cycle elliptically polarized laser pulse by carrier-envelope-phase. Opt Express. 2016;24(7):7525.
[22] Bergues B, Kübel M, Johnson NG, Fischer B, Camus N, Betsch KJ, et al. Attosecond tracing of correlated electron-emission in non-sequential double ionization. Nat Commun. 2012;3(1):813.
[23] Maxwell AS, Faria CFdeM. Controlling below-threshold nonsequential double ionization via quantum interference. Phys Rev Lett. 2016;116(14):143001.
[24] Ye D, Li M, Fu L, Liu J, Gong QH, Liu YQ, et al. Scaling laws of the two-electron sum-energy spectrum in strong-field double ionization. Phys Rev Lett. 2015;115(12):123001.
[25] Hao JX, Hao XL, Li WD, Hu SL, Chen J. Controlling three-dimensional electron–electron correlation via elliptically polarized intense laser field. Chin Phys Lett. 2017;34(4):043201.
[26] Huang C, Guo W, Zhou Y, Wu Z. Role of coulomb repulsion in correlated-electron emission from a doubly excited state in non-sequential double ionization of molecules. Phys Rev A. 2016;93(1):013416.
[27] Liu YQ, Fu LB, Ye DF, Liu J, Li M, Wu CY, et al. Strong-field double ionization through sequential release from double excitation with subsequent coulomb scattering. Phys Rev Lett. 2014;112(1):013003.
[28] Xu TT, Chen JH, Pan XF, Zhang HD, Ben S, Liu XS. Effect of elliptical polarizations on nonsequential double ionization in two-color elliptically polarized laser fields. Chin Phys B. 2018;27(9):093201.
[29] Ben S, Guo PY, Pan XF, Xu TT, Song KL, Liu XS. Recollision induced excitation-ionization with counter-rotating two-color circularly polarized laser field. Chem Phys Lett. 2017;679:38–44.
[30] Eckart S, Richter M, Kunitski M, Hartung A, Rist J, Henrichs K, et al. Nonsequential double ionization by counterrotating circularly polarized two-color laser fields. Phys Rev Lett. 2016;117(13):133202.
[31] Mancuso CA, Dorney KM, Dorney DD, Chaloupka JL, Ellis JL, Dollar FJ, et al. Controlling nonsequential double ionization in two-color circularly polarized femtosecond laser fields. Phys Rev Lett. 2016;117(13):133201.
[32] Chaloupka JL, Hickstein DD. Dynamics of strong-field double ionization in two-color counterrotating fields. Phys Rev Lett. 2016;116(14):143005.
[33] Li BQ, Yang X, Ren XH, Zhang JT. Enhanced double ionization rate from O2 molecules driven by counter-rotating circularly polarized two-color laser fields. Opt Express. 2019;27(22):32700–08.
[34] Peng M, Bai LH, Guo Z. Influence of relative phase on nonsequential double ionization process of CO_2 molecules by counter-rotating two-color circularly polarized laser fields. CommunTheorPhys. 2021;73(7):075501.
[35] Su J, Liu ZC, Liao JY, Huang XF, Li YB, Huang C. Electron correlation and recollision dynamics in nonsequential double ionization by counter-rotating two-color elliptically polarized laser fields. Opt Express. 2022;30(14):24898.
[36] Panfili R, Eberly JH, Haan SL. Comparing classical and quantum dynamics of strong-field double ionization. Opt Express. 2001;8(7):431.
[37] Haan SL, Breen L, Karim A, Eberly JH. Variable time lag and backward ejection in full-dimensional analysis of strong-field double ionization. Phys Rev Lett. 2006;97(10):103008.
[38] Xu TT, Ben S, Wang T, Zhang J, Guo J, Liu XS. Exploration of the nonsequential double-ionization process of a Mg atom with different delay time in few-cycle circularly polarized laser fields. Phys Rev A. 2015;92(3):033405.
[39] Huang C, Zhong M, Wu Z. Intensity-dependent two-electron emission dynamics in nonsequential double ionization by counter-rotating two-color circularly polarized laser fields. Opt Express. 2018;26(20):26045.
[40] Zhu QY, Xu TT, Ben S, Chen JH, Song KL, Liu XS The carrier-envelope phase effect in non-sequential double ionization by few-cycle linearly polarized laser field. Opt Commun 2018;426:602–6.